

Stripe Domains and First-Order Phase Transition in the Vortex Matter of Anisotropic High-Temperature Superconductors

V. K. Vlasko-Vlasov,¹ J. R. Clem,² A. E. Koshelev,¹ U. Welp,¹ and W. K. Kwok¹

¹*Materials Science Division, Argonne National Laboratory, Argonne, Illinois 60439, USA*

²*Department of Physics and Astronomy, Iowa State University, Ames, Iowa 50011-3160, USA*

(Received 27 October 2013; published 17 April 2014)

We report the direct imaging of a novel modulated flux striped domain phase in a nearly twin-free YBCO crystal. These domains arise from instabilities in the vortex structure within a narrow region of tilted magnetic fields at small angles from the in-plane direction. By comparing the experimental and theoretically derived vortex phase diagrams we infer that the stripe domains emerge from a first-order phase transition of the vortex structure. The size of domains containing vortices of certain orientations is controlled by the balance between the vortex stray field energy and the positive energy of the domain boundaries. Our results confirm the existence of the kinked vortex chain phase in an anisotropic high temperature superconductor and reveal a sharp transition in the state of this phase resulting in regular vortex domains.

DOI: [10.1103/PhysRevLett.112.157001](https://doi.org/10.1103/PhysRevLett.112.157001)

PACS numbers: 74.25.Uv, 74.25.Dw, 74.25.Ha, 75.60.Ch

In type II superconductors (SC) the magnetic field penetrates in the form of vortices—magnetic flux tubes each carrying a single flux quantum [1]. Interactions between vortices and their coupling to crystal defects result in a rich variety of vortex structures. They include a triangular or square vortex lattice that can subsequently melt at high temperatures to a vortex liquid, a pinned vortex glassy state that can sustain high current carrying capacity, and in highly anisotropic superconductors, 2D pancake vortices that can interact with in-plane Josephson vortices to create 1D vortex chain states. These states of vortex matter define all transport and magnetic properties of applied superconductors.

Here we report on an unusual vortex domain structure that arises following a first-order phase transition in the vortex state in nearly untwined YBCO crystal under tilted magnetic fields. Typically, vortices repulse each other when the distance between them is much smaller than the penetration depth λ , the scale over which the magnetic field of the vortices decays. In this case, the vortices can arrange into a uniformly spaced lattice or form smooth density gradients defined by the critical current, the maximum current that the superconductor can sustain before reverting to the normal state. In contrast, at larger distances the interactions between vortices can be attractive, resulting in the formation of vortex chains and bundles (see review [2]). For example, periodic stripe domains and circular bundles of vortices interspersed with flux free Meissner regions occur in thin niobium disks with a low Ginzburg-Landau parameter $\kappa = \lambda/\xi \sim 1$, where ξ is the coherence length setting the size of the vortex core. These vortex domains are similar to the alternating normal (N) and superconducting Meissner (M) domains found in the intermediate state of type I SCs with a nonzero

demagnetizing factor. In the latter, the lamellae M/N domains are known to minimize the magnetostatic energy of the normal regions at the expense of the positive energy of the boundaries between the normal and SC phases.

Vortex attraction can also appear in large κ , anisotropic type II SCs when an applied magnetic field is tilted from the anisotropy axis [3–5]. Here, the circulating supercurrents that form the vortex tend to flow perpendicular to the anisotropy axis rather than to the vortex line. This creates an inversion of the magnetic field at some distance from the vortex core resulting in an attraction of the neighboring vortex within the tilt plane [3,5] and formation of dense vortex chains coexisting with the dilute lattice of Abrikosov vortices, as observed in decoration, Hall probe, and electron microscopy experiments in layered high- T_c superconductors (see review [6]).

The formation of patterns including stripe structures is a general phenomenon for a wide variety of condensed matter and colloidal systems with competing attractive and repulsive interactions acting at different length scales [7–9]. In fact, long range attraction and short range repulsion of vortices in superconductors with two order parameters [10] and in multilayers composed of different superconductors [11,12] can result in the formation of vortex stripes. Experimentally, stripes of vortices entwined with the Meissner phase were observed in the two-band superconductor MgB_2 [13,14] and were treated as a possible consequence of the two different superconducting condensates.

In this work we discovered a new vortex structure of regular stipe domains with alternating flux density B_z generated by magnetic fields tilted from the ab plane in a nearly twin-free YBCO platelet crystal. Unlike vortex or Meissner domains and vortex chain structures, our vortex

domains are created via an instability in the vortex state [15–22] due to a first-order phase transition characterized by an abrupt jump in the vortex tilt angle [23]. A possibility of such first-order transition in the vortex orientation was first noticed by Buzdin and Simonov in [24]. During the phase transition, an intermediate state with domains of different vortex phases (orientations) emerges. We propose that similar to the case of type I SCs and ferromagnets, the regular structure of domains with alternating density of B_z reduces the magnetostatic energy of the vortex stray fields perpendicular to the surface of the sample. Between the domains with different flux orientations vortices gradually rotate forming a domain boundary. Responsible for this rotation supercurrents yield a positive domain wall energy which limits the refinement of domains caused by magnetostatics. We suggest that the attractive coupling of tilted vortices into chains along the vortex tilt plane [3–5] and attraction between the neighboring chains with mutually shifted vortices stabilizes domains with larger B_z . Our calculated vortex structure phase diagram in tilted fields defines the boundaries of the angular vortex instability in YBCO in qualitative agreement with the experiment.

The $\text{YBa}_2\text{Cu}_3\text{O}_{7-\delta}$ rectangular platelet crystal ($1130 \times 340 \times 20 \mu\text{m}^3$) used in our experiments was grown using a flux method. The crystal had a few narrow twin lamellae near one end but most of the area was twin free. The onset temperature of the superconducting transition and the width were $T_c = 92.4$ K and $\Delta T = 0.3$ K, respectively, as determined from magnetization measurements. We imaged the perpendicular magnetic fields (B_z) on the sample surface using a magneto-optical (MO) indicator technique [25]. Data were obtained after cooling the sample in applied magnetic fields tilted from the ab plane of the crystal as well as during remagnetization of the sample in tilted fields. The resulting intensity of the MO images depicts the strength and polarity of the normal field B_z .

Figure 1(a) delineates the spatial field pattern at $T = 60$ K after cooling the sample in a field of $H_{\parallel} = 1388$ Oe parallel to the long edge of the sample and then switching off the field. The dark (negative B_z) and bright (positive B_z) image contrast on the right and left edges of the sample demonstrates that trapped vortices induced by the applied field lie parallel to the sample plane and their ends produce stray fields that diverge up at the left edge and converge down at the right edge, as shown in Fig. 1(d). Similar images were observed when H_{\parallel} was tilted by less than $\sim 0.5^\circ$ from the sample plane.

At tilt angles $> 0.5^\circ$ a qualitatively new stripe pattern emerges at the center of the sample. Figure 1(b) shows such a pattern formed after cooling the sample in a field $H_{\parallel} = 1388$ Oe with a tilt angle of $\sim 1.6^\circ$ and switching off the field. Similar to Fig. 1(a) there is bright and dark contrast at the short sample ends and a new dark contrast appears at the top and bottom long edges of the crystal. The latter is

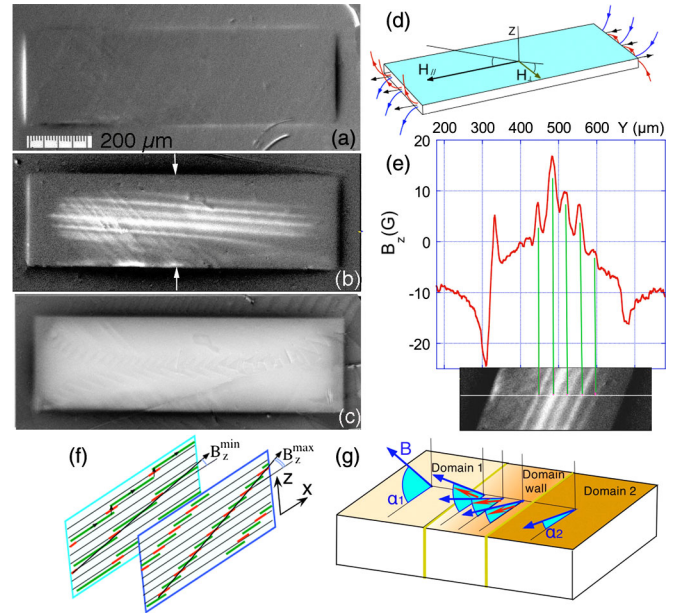


FIG. 1 (color online). (a) Trapped flux ($H = 0$) after field cooling from $T > T_c$ to 60 K in $H_{\parallel} = 1388$ Oe. (b) Same after cooling in $H = 1388$ Oe tilted by 1.6° . Stripe domains are not exactly parallel to the long sides of the sample due to a small misalignment of the field. Domains are also distorted due to the sample edges and defects. (c) Same after cooling in $H = 1388$ Oe tilted by 3.5° . (d) Scheme of the stray fields corresponding to (a). (e) B_z profile across the sample between arrows shown in (b). Spatial resolution of the MOI technique is $2 \mu\text{m}$. (f) Scheme of the staircase vortices in cuprates. (g) Scheme of the vortex domains. Currents (short arrows) in the domain wall flow along vortices in force free configuration.

associated with negative stray field around the sample due to the positive B_z trapped in the central region of the sample. It is in this region the periodic stripes with alternating B_z values reside. Figure 1(e) shows the B_z profile measured across the stripes. It clearly reveals periodic oscillations of B_z superimposed on a monotonic spatial induction gradient. The latter is typical of perpendicular trapped flux in a superconducting plate and corresponds to the average critical current circulating in the ab plane of the sample [26–28]. We associate the observed stripe pattern with a domain structure of vortices with different tilt angles or, equivalently, with different density of in-plane and c -axis vortex segments within the vortex staircase structure inherent for cuprates [29,30,19,23] [see Fig. 1(f)]. This novel domain structures exist in a narrow range of tilt angles between $\theta \sim 0.5$ and 2.4° . Within this range, the width and length of the trapped B_z region and thus the length of the stripe domains were slightly shorter for smaller angles. At a fixed angle the trapped B_z region was shorter for smaller fields. Figure 2 depicts the phase diagram of the observed stripe domain structures obtained by cooling the sample to 60 K under

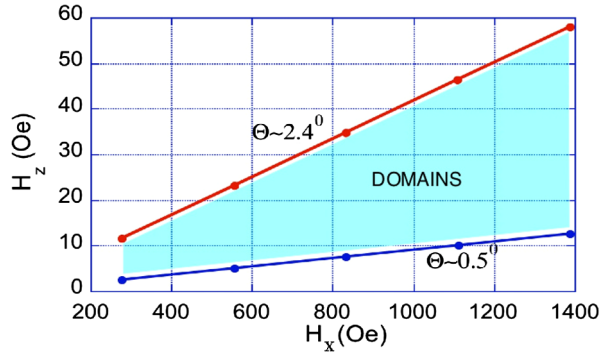


FIG. 2 (color online). Experimental H_z - H_x domain existence map. The map is obtained by imaging vortex structures after tilting the field coils to different angles Θ and cooling at different field values at each angle followed by switching off the field. The novel vortex domains were observed within the range of angles and fields shown in the figure.

various angles of applied fields H_{\parallel} ranging from ~ 280 to 1388 Oe.

To track the initial stage of the domain nucleation we imaged the flux structure during gradual reduction of the field after initially field cooling the sample to $T = 60$ K with $H_{\parallel} = 1388$ Oe tilted by 1.6° (see MO pictures in the Supplemental Material [31]). Before reducing H_{\parallel} , the B_z distribution is homogeneous over the entire imaged area. Decreasing the field to ~ 900 Oe results in the appearance of a dark edge contrast due to the stray fields coming from the trapped positive B_z . Simultaneously, stripes of alternating bright and dark contrast (modulated B_z) emerge along H_{\parallel} near short ends of the sample. Further decreasing the magnetic field extends the stripes over the entire length of the sample. At even smaller $H_{\parallel} \sim 150$ Oe, vortices turn into the plane near the perimeter of the sample and a region of trapped B_z with stripe domains forms inside the crystal. This configuration remains after reducing the field to zero. For angles larger than 2.4° the field cooling resulted in a larger region of stronger trapped B_z but without any stripe domain features [Fig. 1(c)].

The nucleation of domains could be also initiated if after cooling in $H_{\parallel} = 1388$ Oe the field was first increased by a few hundred gauss and then decreased back to the initial value. After field cooling the MO picture was homogeneous. But after increasing and decreasing field back to 1388 Oe, stripes appeared at the short ends of the sample. They extended over the central area during further reduction of H_{\parallel} as described above.

Similar observations were also performed in tilted fields $H_{\perp}(\theta_{\perp})$ perpendicular to the long sample side. In this case the stripe domains formed along the width of the sample and were wider and somewhat less regular than in H_{\parallel} [Fig. 3(a)]. They also exist in a narrow range of tilt angles ($\theta_{\perp} \sim 0.4$ to 3°) and become shorter with decreasing θ_{\perp} [Fig. 3(b)]. At smaller angles the total trapped B_z is weaker and black and white contrast at the long edges of the crystal

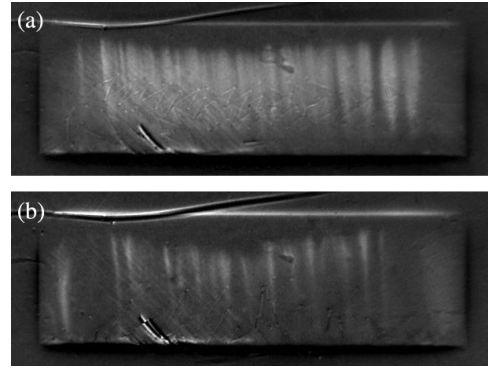


FIG. 3 Vortex domains at 60 K after application and switching off $H_{\perp} = 2100$ Oe along the short side tilted from the ab plane by $\sim 1.2^\circ$ (a) and $\sim 0.4^\circ$ (b). Effect of the sample edges on the domain distortion is stronger in (b).

appears due to the stronger in-plane flux B_y . The domains emerge in the shape of narrow wedges stretching along H_{\perp} from the long edges during application of large enough field. At decreasing field they detach from the edges and remain in the central region after switching H_{\perp} off.

So far there were no experimental reports of vortex domains in high- κ SCs, although the coexistence of vortex lattices with different tilt angles could be expected from theoretical predictions of vortex angle instabilities. These instabilities were calculated for some range of angles for (i) a single tilted vortex line in anisotropic three-dimensional superconductors [15–17,20–22], (ii) a single tilted vortex line in layered superconductor with purely magnetic coupling [19], and (iii) a chain of tilted vortex lines [23]. Below, we derive the vortex phase diagram for YBCO under tilted magnetic fields by taking into account the energy of individual vortices and energies of their interactions and their coupling to external fields. We then analyze the stray fields in thin SC plates and show that they define the width of the stripe domains and discuss vortex attraction as a possible mechanism for stabilizing domains with larger B_z .

The vortex phase diagram in tilted fields is constructed using analytic results for vortex-chain energies derived in Ref. [23] (see [31] for details). Our calculations for a bulk sample show abrupt changes in the vortex angle which are mostly driven by the energy of an isolated vortex chain formed in the tilt plane while interactions between the chains may be neglected. The total energy of a vortex chain E_{TV} consists of isolated vortex line and intervortex coupling contributions, $E_{TV} = E_{TV^i} + E_{TV^i}$. Both terms depend on the in-plane and c -axis magnetic field components and on the SC materials parameters including anisotropy γ [31]. The structure of vortices tilted by a small angle from the in-plane direction $\theta < 1/\gamma$ can be described by the addition of c -axis pancake vortices (kinks) to the Josephson vortex line lattice in purely in-plane field. The equilibrium state is obtained by minimizing the sum of

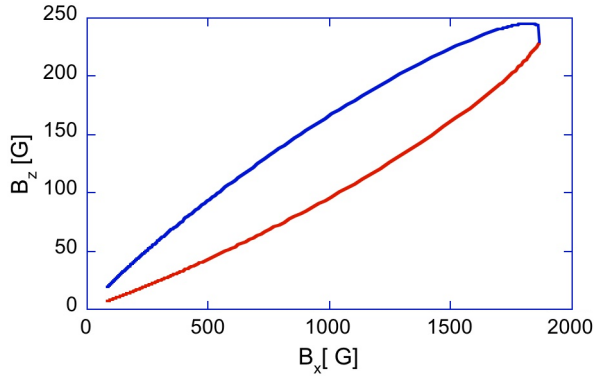


FIG. 4 (color online). Calculated phase diagram of the vortex state in YBCO under tilted fields. With increasing tilt, the B_z component jumps from the bottom to top line. The intermediate state domains should form in the area between the lines.

E_{TV} and the energy of interaction of the c -axis flux with thermodynamic magnetic field H_z . We found that in some range of parameters the total energy has minima at two values of B_z and the system undergoes a first-order phase transition at the critical value of H_z resulting in a jump in B_z . Roughly, the transition is located in the in-plane field range $B_x < \gamma\Phi_0^2/\lambda_{ab}^2$ and bypassed range of B_z corresponds to tilt angles around $\theta \sim 1/\gamma$. Figure 4 shows numerically computed phase diagram obtained for typical YBCO parameters, the penetration depth $\lambda_{ab} = 200$ nm, distance between CuO_2 layers $s = 1.2$ nm, and anisotropy $\gamma = 7$. In the region between two lines in Fig. 4 the vortex structure experiences an angular instability and the c -axis component of the flux, B_z , jumps from B_z^{\min} to B_z^{\max} via a first-order phase transition. Although the sample shape and vortex pinning are not accounted for in this theory, the calculated phase diagram is in reasonable agreement with our experimental H_z - H_x data of the emergence of the stripe domains (Fig. 2). The experimental H_z fields limiting the domain existence are somewhat smaller compared to B_z of the theoretical instability lines. We attribute this difference to the demagnetization factor of the sample and infer the angular vortex instability accompanying the vortex angle transition as the main reason for the appearance of domains.

In large SC samples the sum of energies of individual vortices and bulk vortex-vortex interactions is the main factor defining the flux state. However, in thin SC plates the external stray fields induced by vortices come into play. First, they define the long-range vortex interactions near the surface, which can be treated as a repulsion of magnetic monopoles [32]. Second, they can introduce modulated flux structures, which would reduce the energy of the vortex stray fields around the superconductor (E_s). In type I SCs and low- κ materials this energy is responsible for the emergence and size of the SC/ N or Meissner-Shubnikov lamella domain structures [2]. We conjecture that the regularity of our vortex stripe domain structure can also be explained by the effect of the stray field energy E_s .

Similar to the case of ferromagnetic domains, E_s can be minimized by periodic oscillations of B_z . In relatively small fields, we can consider our system as comprised of up and down magnetized domains superimposed onto an averaged trapped field background. The latter is not important for the variational problem. Formulas for the stripe domains give $E_s \sim 1.7\mu_0^{-1}(\Delta B_z/2)^2 D$ [33]. Here ΔB_z is the difference of B_z in neighboring domains and D is the domain width. An important factor limiting the refinement of domains is the positive energy at their boundaries σ_B . The balance between the reduction of the stray field energy and the increase of the boundary energy yields the equilibrium size of the domains. Positive σ_B is produced by currents responsible for the rotation of vortices in the boundary layer between domains with different flux direction. For example, let us consider two infinite blocks of vortices of the same density B_0 turned by an angle α_0 [α_1 - α_2 in Fig. 1(f)] with a x_0 -thick boundary between them where B_0 rotates in a force-free way [$\mathbf{J}(x) \parallel \mathbf{B}(x)$], so that $\mathbf{B}(x) = \hat{y}B_0\sin[\alpha(x)] + \hat{z}B_0\cos[\alpha(x)]$. The current $\mathbf{J}(x)$ flows only within the boundary layer and vanishes in the homogeneous domains. In the boundary region the current density is $J(x) = \mu_0^{-1}B_0(d\alpha(x)/dx)$. For a linear variation of the vortex angle $\alpha(x) = x(\alpha_0/x_0)$, the force-free current $J(x)$ has some maximum density $J_{c\parallel}$ with the kinetic energy density $\mu_0\lambda^2 J_{c\parallel}^2/2$. The resulting energy per unit area of the boundary will be $\sigma_B = (J_{c\parallel}B_0\alpha_0\lambda^2/2) > 0$. Obviously, the real structure of the boundary is more complex, but the energy due to the boundary currents should still be positive. Minimizing the energy per unit area of the plate $E_s + E_B = 1.7\mu_0^{-1}(\Delta B_z/2)^2 D + \sigma_B(d/D)$, where d is the thickness of the sample, yields the equilibrium size of the stripe domains, $D = (4\mu_0 d \sigma_B / 1.7 \Delta B_z^2)^{1/2}$. Remarkably, this simple formula gives the domain width $D = 30 \mu\text{m}$ (for $d = 20 \mu\text{m}$, $J_{c\parallel} = 10^7$ A/cm 2 , $\alpha_0 = 2^\circ$, $\lambda = 200$ nm, and $\Delta B_z = 10$ G) very close to the observed values ($D \sim 20 \mu\text{m}$).

One could expect that in the increased B_z domains there is an enhanced repulsion of vortices. However, we suggest that the vortex attraction in the chains along the tilt plane and attraction between the chains can stabilize these domains. For a linear chain of tilted vortices the intrachain attraction emerges through the pancake components of vortices and has a dipolar character [34]. The same dipolar attraction can occur between the chains if pancake stacks in the neighboring chains are shifted by half-a-period along the chain. A possible confirmation of this scenario could be zigzag vortex chains observed in NbSe_2 in fields close to the basal plane [35]. This mechanism can also account for the formation of chain bundles in BSCCO in fields strongly tilted from the c axis [36].

In summary, we report the first direct imaging of a novel vortex stripe domain phase in a nearly twin-free YBCO crystal. The domains with alternating B_z arise from instabilities in the vortex state within a narrow region of

tilted magnetic fields at small angles from the ab plane. By comparing the experimental and theoretically derived vortex phase diagrams we infer that the stripe domains emerge due to a first-order phase transition of the vortex structure. We show that the size of domains with different vortex angles is defined by the balance of the vortex stray field energy and positive energy of domain boundaries. Our results confirm the emergence of the kinked vortex chain phase in an anisotropic high temperature superconductors and reveal sharp transformations in their state.

This work was supported by the U.S. Department of Energy, Office of Science, Materials Sciences and Engineering Division. One of us (J.R.) acknowledges support from the Center for Emergent Superconductivity, an Energy Frontier Research Center funded by the U.S. Department of Energy, Office of Science, Office of Basic Energy Sciences.

-
- [1] A. A. Abrikosov, *J. Phys. Chem. Solids* **2**, 199 (1957).
 [2] E. H. Brandt and M. P. Das, *J. Supercond. Novel Magn.* **24**, 57 (2011).
 [3] A. M. Grishin, A. Y. Martynovich, and S. V. Yampolskii, *Zh. Eksp. Teor. Fiz.* **97**, 1930 (1990) [*Sov. Phys. JETP* **70**, 1089 (1990)]; *Physica (Amsterdam)* **165B–166B**, 1103 (1990).
 [4] A. I. Buzdin and A. Yu. Simonov, *Pis'ma Zh. Eksp. Teor. Fiz.* **51**, 168 (1990) [*JETP Lett.* **51**, 191 (1990)].
 [5] V. G. Kogan, N. Nakagawa, and S. L. Thiemann, *Phys. Rev. B* **42**, 2631 (1990).
 [6] S. J. Bending and M. J. W. Dodgson, *J. Phys. Condens. Matter* **17**, R955 (2005).
 [7] G. Malescio and G. Pellicane, *Nat. Mater.* **2**, 97 (2003); *Phys. Rev. E* **70**, 021202 (2004).
 [8] C. J. Olson Reichhardt, C. Reichhardt, and A. R. Bishop, *Phys. Rev. E* **82**, 041502 (2010).
 [9] K. Nelissen, B. Partoens, and F. M. Peeters, *Phys. Rev. E* **71**, 066204 (2005).
 [10] E. Babaev and M. Speight, *Phys. Rev. B* **72**, 180502(R) (2005).
 [11] L. Komendova, M. V. Milosevic, and F. M. Peeters, *Phys. Rev. B* **88**, 094515 (2013).
 [12] C. N. Varney, K. A. H. Sellin, Q.-Z. Wang, H. Fangohr, and E. Babaev, *J. Phys. Condens. Matter* **25**, 415702 (2013).
 [13] V. V. Moshchalkov, M. Menghini, T. Nishio, Q. H. Chen, A. V. Silhanek, V. H. Dao, L. F. Chibotaru, N. D. Zhigadlo, and J. Karpinski, *Phys. Rev. Lett.* **102**, 117001 (2009).
 [14] J. Gutierrez, B. Raes, A. V. Silhanek, L. J. Li, N. D. Zhigadlo, J. Karpinski, J. Tempere, and V. V. Moshchalkov, *Phys. Rev. B* **85**, 094511 (2012).
 [15] A. Sudbo, E. H. Brandt, and D. A. Huse, *Phys. Rev. Lett.* **71**, 1451 (1993).
 [16] L. L. Daemen, L. J. Campbell, A. Yu. Simonov, and V. G. Kogan, *Phys. Rev. Lett.* **70**, 2948 (1993).
 [17] E. Sardella and M. A. Moore, *Phys. Rev. B* **48**, 9664 (1993).
 [18] G. Preosti and P. Muzikar, *Phys. Rev. B* **48**, 9921 (1993).
 [19] M. Benkraouda and J. R. Clem, *Phys. Rev. B* **53**, 438 (1996).
 [20] A. K. Nguyen and A. Sudbo, *Phys. Rev. B* **53**, 843 (1996).
 [21] A. M. Thompson and M. A. Moore, *Phys. Rev. B* **55**, 3856 (1997).
 [22] P. Muzikar, *J. Low Temp. Phys.* **115**, 135 (1999).
 [23] A. E. Koshelev, *Phys. Rev. B* **71**, 174507 (2005).
 [24] A. I. Buzdin and Yu. A. Simonov, *Supercond. Sci. Technol.* **5**, s284 (1992).
 [25] V. K. Vlasko-Vlasov, U. Welp, G. W. Crabtree, and V. I. Nikitenko, in *Physics, and Materials Science of Vortex States, Flux Pinning, and Dynamics*, NATO Advanced Study Institute, Series E: Applied Sciences Vol. 356, edited by R. Kossowsky *et al.* (Kluwer, Dordrecht, 1999), pp. 205–237.
 [26] P. N. Mikheenko and Yu. E. Kuzovlev, *Physica (Amsterdam)* **204C**, 229 (1993).
 [27] E. H. Brandt and M. Indenbom, *Phys. Rev. B* **48**, 12 893 (1993).
 [28] E. Zeldov, J. R. Clem, M. McElfresh, and M. Darwin, *Phys. Rev. B* **49**, 9802 (1994).
 [29] B. I. Ivlev, Y. N. Ovchinnikov, and V. L. Pokrovskii, *Mod. Phys. Lett. B* **05**, 73 (1991).
 [30] L. N. Bulaevskii, M. Ledvij, and V. G. Kogan, *Phys. Rev. B* **46**, 366 (1992).
 [31] See Supplemental Material at <http://link.aps.org/supplemental/10.1103/PhysRevLett.112.157001> for details of calculation of the phase diagram in tilted fields.
 [32] G. Carneiro and E. H. Brandt, *Phys. Rev. B* **61**, 6370 (2000).
 [33] L. D. Landau and E. M. Lifshitz, *Electrodynamics of Continuous Media* (Pergamon, Oxford, 1984).
 [34] A. Buzdin and I. Baladić, *Phys. Rev. Lett.* **88**, 147002 (2002).
 [35] H. F. Hess, C. A. Murray, and J. V. Waszczak, *Phys. Rev. Lett.* **69**, 2138 (1992).
 [36] T. Tamegai, H. Aoki, M. Matsui, and M. Tokunaga, *Pramana J. Phys.* **66**, 271 (2006).